

# Buckling Analysis of Eccentrically Loaded Cracked Columns

L. Nobile<sup>1</sup> and C. Carloni<sup>1</sup>

**Abstract:** The analysis of buckling of elastic columns is one of the first problem in structural engineering that was historically solved. Critical loads of perfect columns with various end restrains have been derived. Nevertheless, the perfect column is an idealized model. In reality, unavoidable imperfections should be considered. Solutions for transversal disturbing load, crookedness or load eccentricity have been proposed. Another frequent imperfection to be taken into account is the weakness at an interior location due to a partial edge crack. In this paper the influence of this type of imperfection on the critical load is analyzed. The case of the load eccentricity has been also considered. The weakness can be modeled as an internal hinge with a rotational spring. Exact critical loads for various end conditions, crack locations and cross-sections are obtained.

**keyword:** Buckling, Crack, Hinge, Rotational spring, Approximate stress intensity factor, Load eccentricity.

## 1 Introduction

A crack on a structural member introduces a local flexibility that affects its static and dynamic response. The local flexibility of the cracked region of the structural element was put into relation with the crack stress intensity factors (SIFs) [Irwin, 1975; Bueckner, 1958; Westmann and Yang, 1967]. The stress intensity factors were obtained in many cases, and a well-known relationship was discovered between the energy release rate, the stress intensity factors and the compliance of the cracked member. The above relationship was then used to study the stability of the cracked columns (Liebowitz, Vanderveldt and Harris, 1967; Liebowitz and Claus, 1968; Okamura, Liu, Chu and Liebowitz, 1969).

A general method was considered by Okamura, Watanabe and Takano (1973) for extending fracture mechanics through the compliance concept to the analysis of a structure containing cracked members. This paper also shows

some examples of the application adopted for the deformation analysis of the cracked specimens.

Stress intensity factors for many configurations are available. In most cases the results were obtained by means of analytical and numerical methods. In many cases the results were obtained by finite element methods and boundary element methods. Experimental methods have been applied to simple cases in order to determine the fracture toughness  $K_{IC}$  of engineering materials. Solutions for many structural configurations are not available in the handbooks (Tada, Paris and Irwin, 1985). Simple engineering methods which allow a fast but approximate determination of the stress intensity factors are highly valued by design engineers. Remarkably simple methods for approximation of stress intensity factors in cracked or notched beams were proposed by Kienzler and Herrmann (1986) and by Nobile (2000). The former has been based on elementary beam theory estimation of strain energy release rate as the crack is widened into a fracture band, the latter has been based on elementary beam theory equilibrium condition for internal forces evaluated in the cross-section passing through the crack tip, taking in account the stress singularity at the tip of an elastic crack.

The influence of this kind of imperfection on the critical load has been analyzed by Wang, Wang and Tun Myint Aung (2004). The weakness is modeled as an internal rotationally restrained hinge. The rotational spring constant is determined on the basis of the energy released due to the crack and Castigliano's theorem.

In this paper critical loads for a cracked column with various end conditions and crack locations are derived. It is worth noticing the buckling analysis is focused on the plane orthogonal to the crack, neglecting the case of lateral buckling coupled with torsion, that will be developed by the authors in the next.

## 2 Approximate evaluation of the Stress Intensity Factor for Mode-I

Consider a straight beam of constant cross section. The  $z$ -axis coincides with the geometrical axis, and the  $x$ -

<sup>1</sup> DISTART, University of Bologna, Viale Risorgimento 2, 40136 Bologna, Italy.

and y-axes coincide with the principal axes of the cross-section. The beam is under pure bending. Suppose that the presence of an edge crack (of length  $a$ ) at a certain position does not alter the stress resultant on the cross-section passing through the crack. The singular stress distribution at the crack tip takes the form

$$\sigma_z^s = \frac{K_I}{\sqrt{2\pi r}} \quad (1)$$

Keeping in mind the Navier formula applied to the reduced cross-section passing through the crack tip, the normal stress is (Fig. 1)

$$\sigma_z = \frac{M_x}{I_x^*} y \quad (2)$$

where  $M_x$  is bending moment and  $I_x^*$  the moment of inertia of the reduced cross-section. Note that the stress distribution (2) does not take into account the presence of the crack.

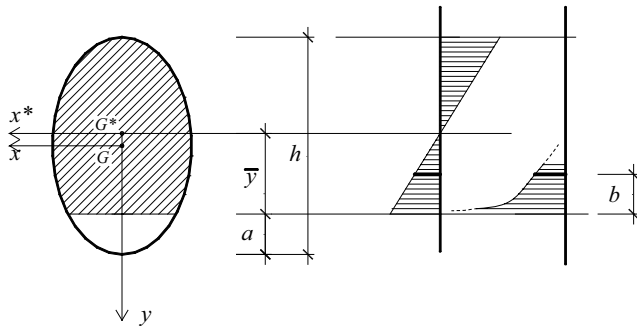


Figure 1 : Cross-section with a crack

Two conditions can be imposed:

1. at a certain distance  $b$  from the crack tip the normal stress due to the Navier formula has to be equal to the normal stress due to the crack (Fig. 1).
2. The stress resultant arising from the crack tip to the distance  $b$ , calculating with the fracture mechanics approach and with the Navier formulation must be equal (Fig. 1).

Making use of the above conditions the distance  $b$  and an approximate stress intensity factor  $K_I$  can be found.

Referring to a rectangular and a T-shape cross-sections (Fig. 2),  $K_I$  becomes respectively:

$$K_I = \frac{6M_x}{Bh^{3/2}} F_I^R(\alpha) \quad (3)$$

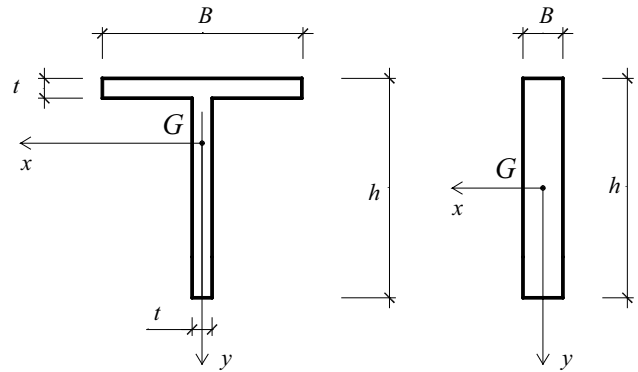


Figure 2 : T-shape and Rectangular cross-sections

$$K_I = \frac{M_x}{h^{5/2}} F_I^T(\alpha, \beta, \tau) \quad (4)$$

where the geometric functions  $F_I^R$  and  $F_I^T$  are reported in Nobile (2000) and Nobile and Carloni (2005). Note that in Eqs. (3) and (4) the following positions have been stated  $\alpha=a/h$ ,  $\beta=B/h$  and  $\tau=t/h$  ( $a$  is the crack length).

### 3 Buckling of a cracked column

Referring to a cracked pin-ended column (Fig. 3a), or to a clamped-pinned column (Fig. 3b), the local flexibility due to the crack is modeled as a massless rotational spring.

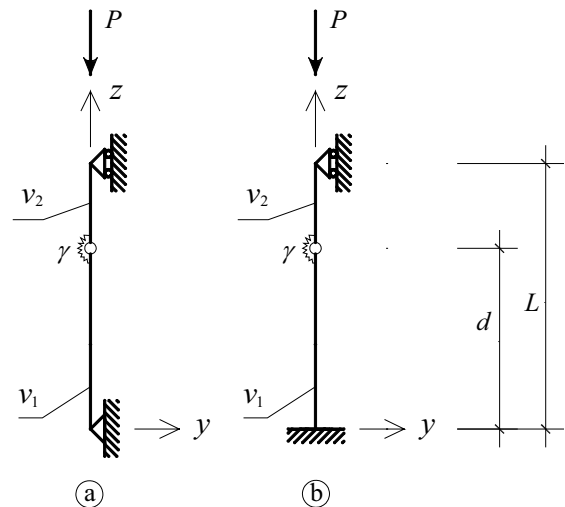


Figure 3 : Model of a crack column

The numerical value of the spring constant  $\gamma$  represents the severity of cracking. It can be simply evaluated from the crack strain energy function (see Section 4).

The governing differential equation for buckling problem of a column under axial load  $P$ , can be written as

$$V^{(IV)}(\zeta) + \lambda^2 V^{(II)} = 0 \quad (5)$$

where  $V = v/L$  is the dimensionless lateral displacement and  $\lambda^2 = PL/EI$ .  $EI$  is the flexural rigidity and  $L$  the length of the column.  $\zeta = z/L$  is the dimensionless coordinate. The solution of the differential equation will be in the form  $V(\zeta) = A_1 \sin(\lambda\zeta) + A_2 \cos(\lambda\zeta) + A_3\zeta + A_4$ .

The crack position is located at  $z = d$ . In what follows the normalized position  $\delta = d/L$  will be used.  $v_1$  and  $v_2$  represent the lateral displacement function for  $0 \leq z \leq d$  and  $d \leq z \leq L$ , respectively. The corresponding normalized function are  $V_1$  and  $V_2$ , with the corresponding normalized range of variation  $0 \leq \zeta \leq \delta$  and  $\delta \leq \zeta \leq 1$ , respectively ( $\delta = d/L$ ).  $V_1$  and  $V_2$  will be used in the following.

For a column with pinned ends  $V_1(0) = 0$ ,  $V_1''(0) = 0$ ,  $V_2(1) = 0$  and  $V_2''(1) = 0$  (see Fig. 3a).

For a clamped-pinned column  $V_1(0) = 0$ ,  $V_1'(0) = 0$ ,  $V_2(1) = 0$  and  $V_2''(1) = 0$  (see Fig. 3b).

At the cracked cross-section the following conditions must be imposed:

$$V_1(\delta) = V_2(\delta) \quad (6)$$

$$V_1''(\delta) = V_2''(\delta) \quad (7)$$

$$V_1'''(\delta) + \lambda V_1'(\delta) = V_2'''(\delta) + \lambda V_2'(\delta) \quad (8)$$

$$V_1''(\delta) = k [V_2'(\delta) - V_1'(\delta)] \quad (9)$$

Eqs. (6) and (7) simply require both the displacement and the bending moment to be continuous. Eq. (8) is related to the continuity of the shear force. Finally Eq. (9) affirms that the bending moment at the junction section is related to the relative rotation. By imposing the ends and the junction conditions a homogenous linear system can be found. The determinant of the coefficients matrix must be set equal to zero to get the characteristic equation.

#### 4 Evaluation of the local flexibility due to the crack

Keeping in mind the Castigliano's theorem (part I), the rotational flexibility of the beam at the crack location can be calculated as:

$$c = \frac{1}{\gamma} = \frac{\partial^2 U}{\partial M^2} \quad (10)$$

where  $U$  is the elastic strain energy caused by the presence of the crack:

$$U = \frac{1}{E} \int_A (K_I^2 + K_{II}^2) dA \quad (11)$$

with  $A$  the area of the crack,  $K_I$  the stress intensity factor for Mode-I and  $E$  the Young modulus.

Since  $K_{II}$  is related only to the shear force,  $U$  reduces to:

$$U = \frac{1}{E} \int_A (K_I^2) dA = \frac{36M^2}{Bh^3E} \int_0^a (F_I^R)^2(\alpha) da \quad (12)$$

$$U = \frac{1}{E} \int_A (K_I^2) dA = \frac{M^2 d}{h^5 E} \int_0^a (F_I^T)^2(\alpha, \beta, \delta) da \quad (13)$$

whether a rectangular or a T-shape cross-section has been considered, respectively.

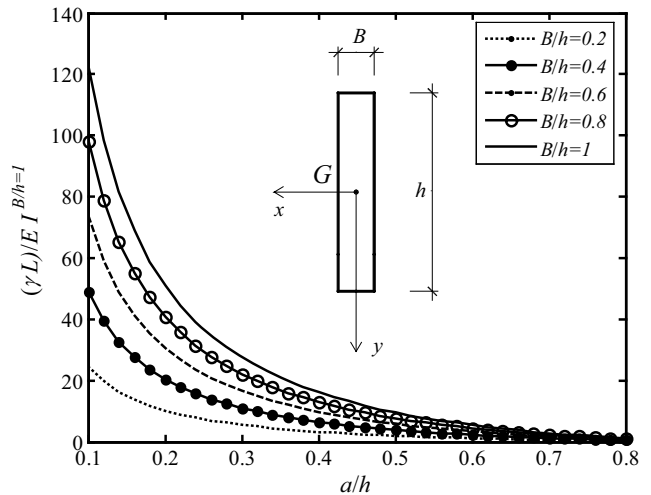


**Figure 4** : Local Flexibility due to the crack for a rectangular cross-section ( $h=100$ )

A plot of the normalized junction stiffness parameter  $k = \gamma L/EI$  as a function of normalized crack length  $a/h$  is shown in Figs. 4 and 5, for the rectangular and T-shape cross-sections, having the same height and moment of inertia. The moment of inertia used to normalized the values of  $\gamma$  is referred to  $B/h=1$  for the rectangular cross-section and to  $B/h=1$  and  $t/h=0.1$  for the T-shape. Note that the local flexibility of the T-shape is not so strongly affected by the width  $B$  and the thickness  $t$  as the rectangular cross-section does with  $B$ .

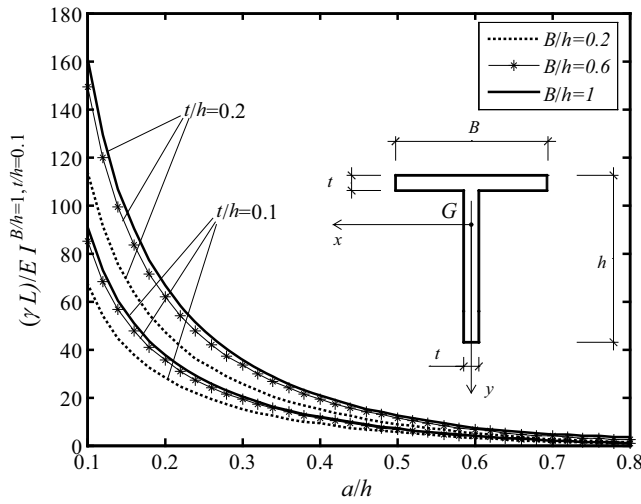


**Figure 5 :** Local Flexibility due to the crack for a T-shape cross-section ( $h=100$ )

### 5 Buckling Loads

Exact critical loads ( $P_{cr}$ ) for various end conditions, crack locations and cross sections are investigated in this Section. Cast Iron has been considered ( $E=175$  GPa;  $K_{IC}=579$  MPa  $\cdot$   $\sqrt{mm}$ ).

#### 5.1 Pin-ended column

Consider the pin-ended column (Fig. 3a). The characteristic equation becomes:

$$\cos(\lambda) - \cos[\lambda(1 - 2\delta)] + \frac{2}{\lambda}k \sin(\lambda) = 0 \quad (14)$$

Figures 6 and 7 show the values of the critical loads normalized respect to the Euler critical load versus the normalized length of the crack, for different position of the crack. The above mentioned figures are referred to the rectangular cross-section and the T-shape cross section, respectively. The cross-sections have the same height ( $h=100$  mm) and the same moment of inertia ( $I=1790000$  mm<sup>4</sup>). Once the crack position is fixed the critical load decreases as the crack length increases. Note that the more the crack tends to the mid-span the more the critical load decreases. Moreover the influence of the section shape is evident as the crack length increases.

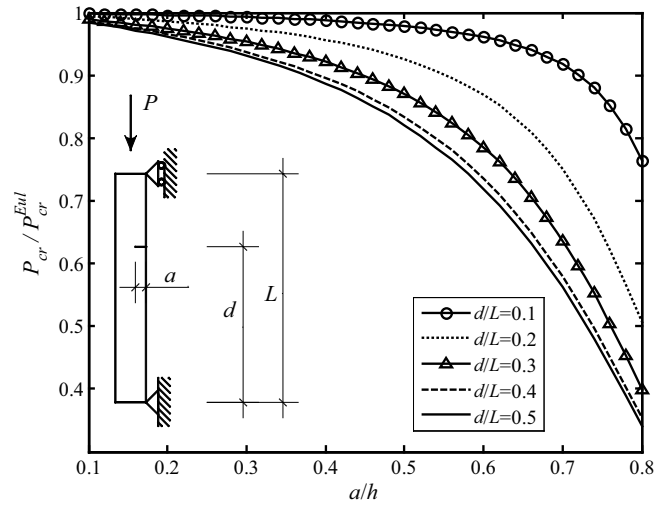


**Figure 6 :** Normalized critical load vs. dimensionless crack length for different crack position (pin-ended column with rectangular cross section)

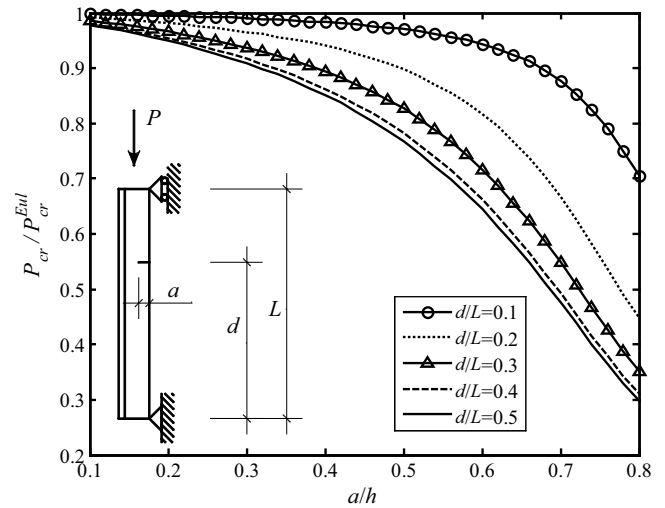


**Figure 7 :** Normalized critical load vs. dimensionless crack length for different crack position (pin-ended column with T-shape cross section)

#### 5.2 Clamped-pinned column

For a column with a clamped end ( $z=0$ ) and the other pinned, the characteristic equation becomes:

$$(1 - 2k)\lambda \cos(\lambda) - \lambda \cos[\lambda(1 - 2\delta)] + (2k + \lambda^2) \sin(\lambda) + \lambda^2 \sin[\lambda(1 - 2\delta)] = 0 \quad (15)$$

Figures 8 and 9 show the values of the critical loads normalized respect to the Euler critical load versus the nor-

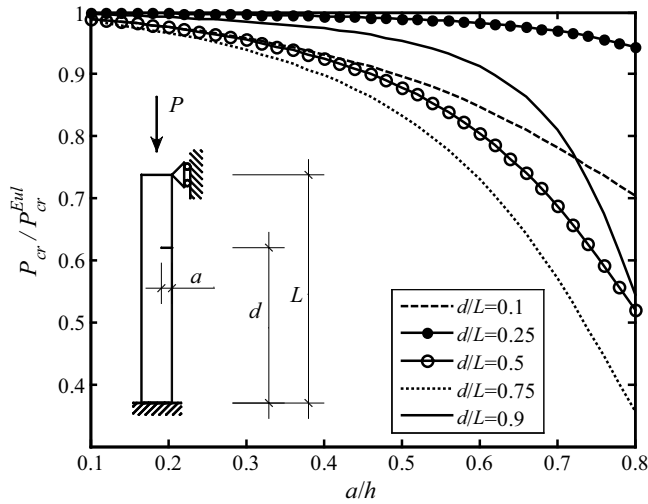


**Figure 8 :** Normalized critical load vs. dimensionless crack length for different crack position (clamped-pinned column with rectangular cross section)

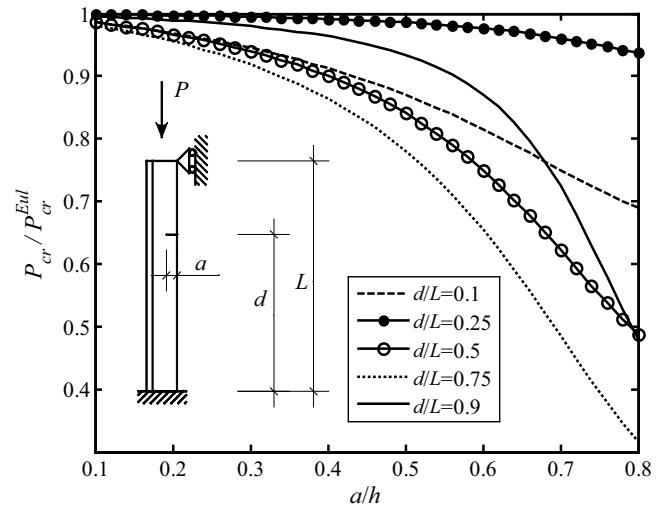


**Figure 9 :** Normalized critical load vs. dimensionless crack length for different crack position (clamped-pinned column with T-shape cross section)

malized length of the crack, for different position of the crack. The above mentioned figure are referred to the rectangular cross section and the T-shape cross section, respectively.

Once again, the cross sections have the same height ( $h=100$  mm) and the same moment of inertia ( $I=1790000$  mm<sup>4</sup>). It can be observed that for  $d/L=0.25$  the critical load seems not be affected by the crack length. This is in accordance with the fact that at  $d/L \cong 0.3$  there is the inflection point for the corresponding perfect Euler column. The critical load decreases as the crack length increases but the influence of the cross section shape is not so evident as in the previous case.

### 6 Load eccentricity

Suppose that the load is applied eccentrically. The eccentricity  $e$  defines the distance of the load from the centroid. If the linearized theory has been taken into account the critical load does not differ from the centered case. By using the appropriate end conditions and Eqs. (6)-(9), the lateral displacement  $V_1$  and  $V_2$  can be obtained as a function of the applied load.

Figure 10 depicts the variation of the lateral displacement at midspan as a function of the applied load for a pin-ended column with a T-shape cross section. As the displacement increases the load becomes asymptotically equal to the corresponding value of the critical load for

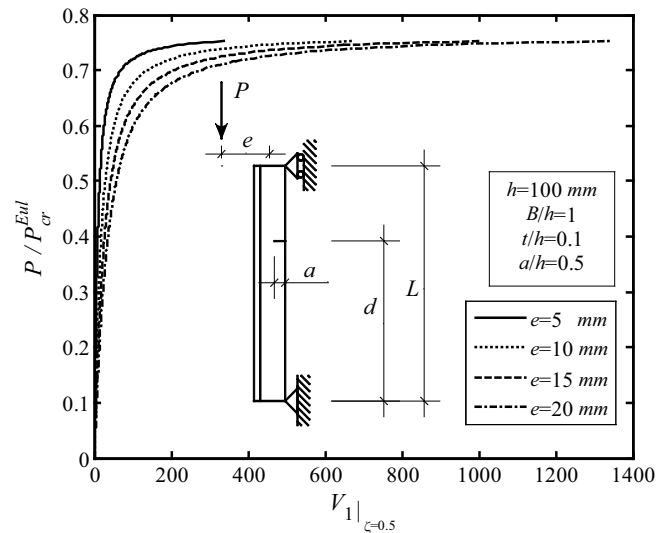


**Figure 10 :** Dimensionless mid-span displacement for pinned column with T-shape cross section as a function of the applied load for different values of the eccentricity  $e$

the centered case.

This is true regardless of the value of the eccentricity. If the load is applied eccentrically the evaluation of the critical load can be vanished by the crack propagation corresponding to a value of the load below the critical one.

Refer to a pin-ended column, with the load applied ec-

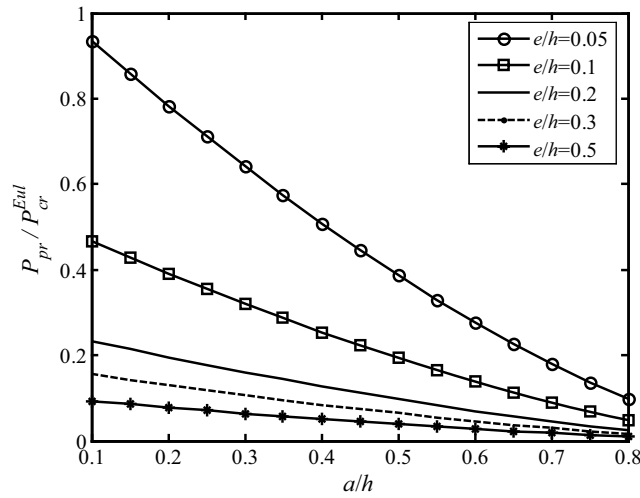


**Figure 11** : Dimensionless propagation load vs. crack length for pinned column, corresponding to different values of eccentricity (rectangular cross section)

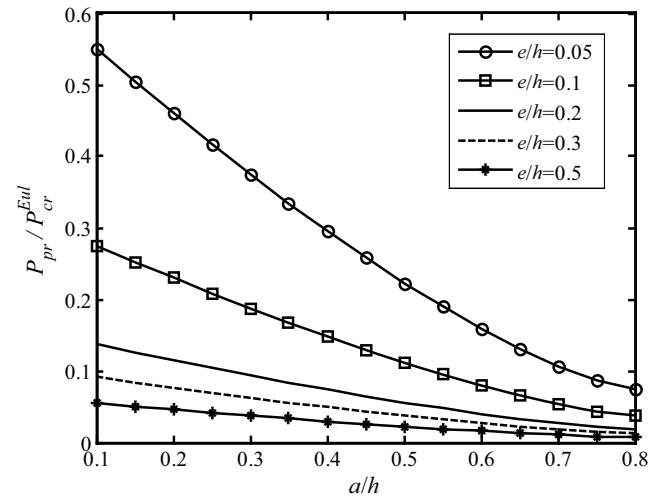


**Figure 12** : Dimensionless propagation load vs. crack length for pinned column, corresponding to different values of eccentricity (T-shape cross section)

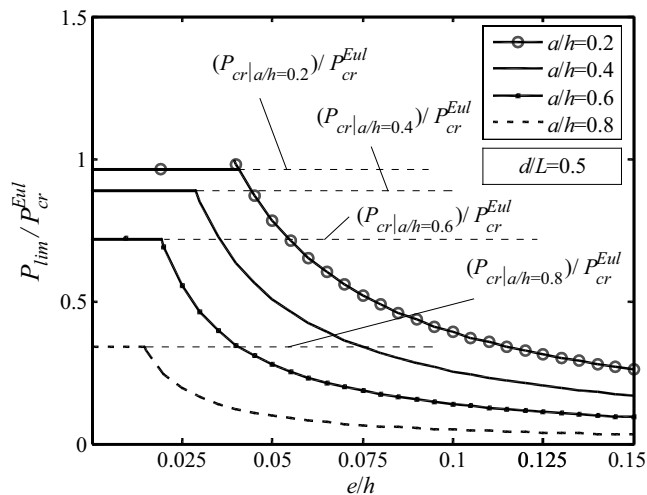


**Figure 13** : Dimensionless limit load vs normalized eccentricity for pinned column, corresponding to different values of crack length (rectangular cross section)

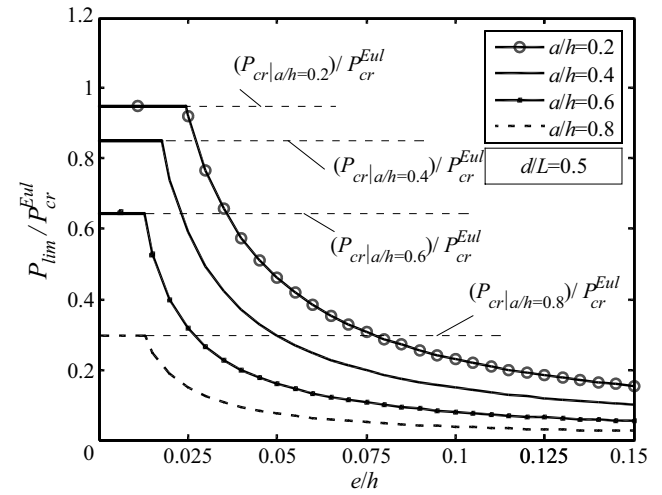


**Figure 14** : Dimensionless limit load vs normalized eccentricity for pinned column, corresponding to different values of crack length (T-shape cross section)

centrically. Let  $P_{cr}$  be the critical load that depends on the cross section, the crack length and position. It can be found by solving the characteristic equation, corresponding to the load applied axially (linearized theory). Define  $P_{pr}$  as the value of the load corresponding to the crack propagation, since the critical value of the stress intensity factor  $K_{IC}$  has been reached. Once the geometric parameters (crack length, crack position, cross section and eccentricity) have been fixed,  $P_{pr}$  can be obtained by

solving the following equations:

$$K_{IC} = \frac{6P_{pr}e}{Bh^{3/2}}F_I^R \tag{16}$$

$$K_{IC} = \frac{P_{pr}e}{h^{5/2}}F_I^T \tag{17}$$

Equations (16) and (17) refer to the rectangular and T-shape cross-sections, respectively.

Figures 11 and 12 depict the values of the propagation load  $P_{pr}$ , normalized respect to the Euler critical load, as

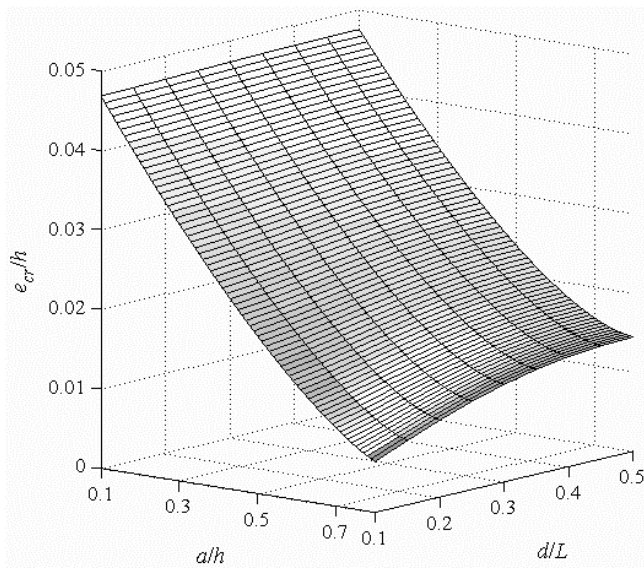


**Figure 15 :** Normalized eccentricity corresponding to the condition (19) for different crack lengths and positions. (rectangular cross section)

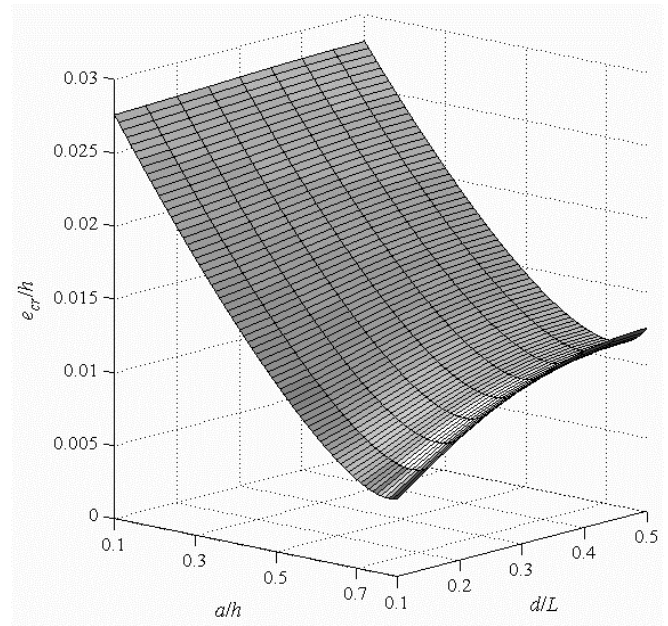


**Figure 16 :** Normalized eccentricity corresponding to condition (19) for different crack lengths and positions. (T-shape)

a function of the dimensionless crack length, for different values of the eccentricity.

As the load is applied eccentrically the critical load has to be compared to the propagation load. The *limit load*  $P_{lim}$  is defined as:

$$P_{lim} = \min \{P_{pr}, P_{cr}\} \quad (18)$$

Referring to a pinned column, figures 13 and 14 show the normalized limit load as a function of the normalized eccentricity, for different crack length and a fixed crack position. The limit load corresponds to the critical load only if the eccentricity is below a certain value depending on the crack length and position. Note that the limit load decreases dramatically as the crack length increases.

Figures 15, 16 and 17 show the critical values of eccentricity  $e_{cr}$  as a function of the normalized crack length ( $a/h$ ) and crack position ( $d/L$ ), corresponding to the following condition:

$$P_{cr} = P_{pr} \quad (19)$$

Note that the surfaces in figures 15 and 16 should be considered as the border surfaces defining the domain of eccentricity where buckling prevails over crack propagation. For the rectangular cross-section (Fig. 17), the eccentricity that fulfills condition (19) decreases as the

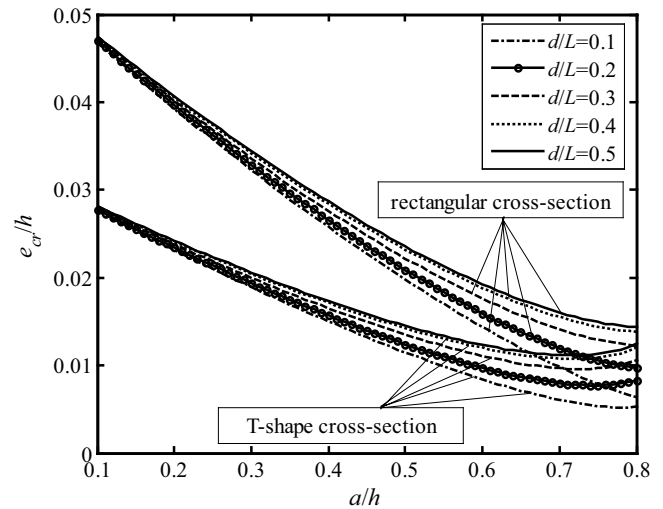


**Figure 17 :** Normalized eccentricity corresponding to condition (19) for different crack lengths and positions.

crack length increases, for a fixed position of the crack. For both cross-sections, as the crack length is fixed,  $e_{cr}$  increases when the crack position moves to the mid-span. Finally (Fig. 17), for a fixed crack position and length,  $e_{cr}$  is greater when a rectangular cross-section is adopted. This fact is emphasized as the crack length decreases.

## 7 Conclusion

In this paper the influence of the presence of an edge crack on the critical load has been analyzed. The weakness due to the crack can be modeled as an internal hinge with a rotational spring. Exact critical loads for various end conditions, crack locations and cross-sections are obtained. Once the crack position is fixed the critical load decreases as the crack length increases. Besides the more the crack tends to the mid span the more the critical load decreases.

The case of the load applied eccentrically has been also considered. If the load is applied eccentrically the evaluation of the critical load can be vanished by the crack propagation corresponding to a value of the load below the critical one. The values of the load eccentricity corresponding to the condition of equivalence between the critical load and the propagation load have been evaluated as a function of the crack length and position.

**Acknowledgement:** Authors gratefully acknowledge the financial support of the Italian Ministry of University and Research.

## References

- Irwin, G.R.** (1975): Analysis of stresses and strains near the end of a crack traversing a plate, *J. Appl. Mech.*, 79, 361-364.
- Bueckner, H.F.** (1958): The propagation of cracks and the energy of elastic deformation, *Trans. ASME*, 80, 1225-1230.
- Westmann, R.A.; Yang, W.H.** (1967): Stress analysis of cracked rectangular beams, *Theor. Appl. Fract. Mech.*, 32, 693-701.
- Liebowitz, H.; Vanderveldt, H.; Harris, D.W.** (1967): Carrying capacity of notched column, *Int. J. Solids Struct.*, 3, 489-500.
- Liebowitz, H.; Claus, W.D.S.** (1968): *Failure of notched columns*, *Eng. Fract. Mech.*, 1, 379-383.
- Okamura, H.; Liu, H.W.; Chu, C.S.; Liebowitz, H.** (1969): A cracked column under compression, *Eng. Fract. Mech.*, 1, 547-564.
- Okamura, H.; Watanabe, K.; Takano, H.** (1973): Applications of the compliance concept in fracture mechanics, *ASTM Spec. Tech. Publ.*, 536.
- Tada, H. Paris, P.C.; Irwin, G.R.** (1985): The stress analysis of cracks handbook, *Del Research Corporation*, Hellertown, Pa.
- Kienzerl, R.; Herrmann, G.** (1986): On the material forces in elementary beam theory, *J. Appl. Mech.*, 53, 561-564.
- Nobile, L.** (2000): Mixed mode crack direction and propagation in beams with edge crack, *Theor. Appl. Fract. Mech.*, 33, 107-116.
- Wang, C.Y.; Wang, C.M.; Tun Myint Aung** (2004): Buckling of a weakened column, *J. Eng. Mech.*, 130, 1373-1376.
- Nobile, L.; Carloni, C.** (2005): Column buckling coupled with fracture, *Proc. IV Inter. Conf. on Fract. and Dam. Mech.*, Mallorca (Spain) July 12-14, 2005, 161-165.